CFD Modeling and Simulation in Materials Processing 2016
Edited by: Laurentiu Nastac, Lifeng Zhang, Brian G. Thomas, Miaoyong Zhu, Andreas Ludwig, Adrian S. Sabau, Koulis Pericleous, and Hervé Combeau
TMS (The Minerals, Metals & Materials Society), 2016

CFD ANALYSIS OF BLAST FURNACE OPERATING CONDITION IMPACTS ON OPERATIONAL EFFICIENCY

Tyamo Okosun, Armin K. Silaen, Guangwu Tang, Bin Wu, and Chenn Q. Zhou

Center for Innovation through Visualization and Simulation
Purdue University Calumet
2200 169th Street
Hammond, IN 46323

Keywords: CFD, Blast Furnace, Combustion, Reacting Flow, Performance Optimization

Abstract

Blast furnaces are counter-current chemical reactors used to reduce iron ore into liquid iron. Hot reduction gases are blasted through a burden consisting of iron ore pellets, slag, flux, and coke. The chemical reactions that occur through the furnace reduce the iron ore pellets into liquid iron as they descend through the furnace. Experimental studies and live operation measurements can be extremely difficult to perform on a blast furnace due to the extremely harsh environment generated by the operational process. Computational Fluid Dynamics (CFD) modeling has been developed and applied to simulate the complex multiphase reacting flow inside a blast furnace shaft. The model is able to predict the burden distribution pattern, Cohesive Zone (CZ) shape, gas reduction utilization, coke rate, and other operational conditions. This paper details the application of this model to investigate the effects of coke size and porosity, iron ore pellet size, and burden descent speed on blast furnace efficiency.

Introduction

The efficiency of a blast furnace can be impacted by several factors. Significantly, the fuel required to operate the furnace at a given production rate of liquid iron can be influenced by the particle size and porosity of the coke charged into the furnace burden and the rate at which the burden descends through the furnace. In order to reduce operational costs, a considerable amount of effort has been made to reduce the coke rate of blast furnaces. A popular method currently in application is coke replacement by injected fuels, such as pulversized coal and natural gas. As injection rates rise to higher levels, it becomes crucial to attain an understanding of the physical phenomena occuring inside the blast furnace shaft. This understanding provides operaters with the ability to optimize the replacement of coke with injected fuels and maintain maximum cost efficiency [1, 2].

Iron ore and coke particles charged into the blast furnace experience gas-solid reactions as they descend through the shaft. The coke solution loss reaction in the shaft of a blast furnace under fixed tuyere operating condtions is the primary determinant of the coke rate. The solution loss can also be characterized as the degree of direct FeO reduction from the coupled reaction of FeO reduction and coke gasification. Because of this coupling, the reaction kinetics of iron ore and coke are interconnected and impact each other as well as the gas flow, thermal conditions, and overall conditions in the blast furnace.

L. Nastac et al. (Eds.), *CFD Modeling and Simulation in Materials Processing 2016*

A previous study examined the impacts of iron ore and coke reducibility on the operation of a blast furnace, finding that increased ore reducibility and low coke reactivity corresponded to decreases in furnace coke rate [3]. In order to manage the reactivity of coke, an examination of coke particle properties is necessary. In general, the size and quality of coke particles charged into blast furnaces are well controlled. However, variations in particle size can occur both unintentionally and intentiontally, leading to varied reduction rates and operating conditions inside the furnace shaft. Given the variety of operating conditions that can occur with increased fuel injection rates below the furnace shaft, it also becomes important to consider the rate at which the burden descends through the shaft. Variations in descent speed lead to radically different burden distributions which can greatly impact flow patterns and, by extension, reaction rates through the furnace shaft.

The research detailed in this paper explores the impacts of coke particle size, ore particle size, coke bed porosity, and burden descent speed on the operation of a blast furnace. An in-house CFD model was utilized to simulate the furnace at various operating conditions for this investigation. Results obtained from this study could provide guidance for the improvement of blast furnace efficiency, reduction of coke consumption, and decreases in CO_2 emissions.

CFD Model

A previously developed in-house CFD code, the blast furnace shaft simulator, was utilitzed to model gas flow and reaction phenomena inside the furnace [3]. The chemical reactions included in this model are detailed in previous publications [4]. The single interface unreacted shrinking core (URC) model is applied to represent iron ore reduction in this CFD simulation [5]. The complex process of iron ore reduction has been simplified to three rate control processes, namely, gas film resistance, diffusion resistance through the reduced iron shell, and intrinsic chemical reaction resistance at the metal-oxide interface. The expression for the reaction rate for one ore particle is expressed as Eq. 1.

$$R_i = \frac{4\pi r_0^2 (C_A - \frac{C_B}{K_{e,i}}) \frac{K_{e,i}}{(1+K_{e,i})}}{F + B_i + A_i} \quad (\frac{mol\ CO}{s}) \quad , i = 1 - 6 \qquad \text{Eq. 1}$$

Where the gas film resistance is: $F = \frac{1}{\beta_A} (\frac{s}{m})$, the diffusion resistance is:

$$B_i = \frac{r_0}{D_{e,i}} [(1 - f_i)^{-\frac{1}{3}} - 1] (\frac{s}{m}), \qquad \text{Eq. 2}$$

the intrinsic chemical reaction resistance is:

$$A_i = \frac{1}{k_i} (1 - f_i)^{-2/3} \frac{K_{e,i}}{(1+K_{e,i})} (\frac{s}{m}), \qquad \text{Eq. 3}$$

and the fraction of reduction f_i is defined as:

$$f_i = \frac{weight\ of\ oxygen\ removed\ from\ iron\ oxide}{weight\ of\ removable\ oxygen}, \qquad \text{Eq. 4}$$

r_0 is the radius of the iron ore, and the effective diffusivity is: $D_{e,i} = D_o \frac{\varepsilon_i}{\tau}$.

The porosities for each layer are [5]:

$$\varepsilon_{HM} = 0.008 + 0.992\varepsilon_o \quad \text{Eq. 5}$$

$$\varepsilon_{MW} = 0.122 + 0.878\varepsilon_o \quad \text{Eq. 6}$$

$$\varepsilon_{WF} = 0.435 + 0.565\varepsilon_o \quad \text{Eq. 7}$$

Where ε_o is the original ore porosity, as charged into the furnace, before any reactions. The tortuosity τ, is assumed to be 2 and $K_{e,i}$ are the equilibrium constants [6]. For each reaction step, the kinetic constant is:

$$k_i = k_{i,o} exp(\frac{-E_i}{RT_s}). \quad \text{Eq. 8}$$

Values for the frequency factors and activation energies for reduction reactions are adopted from prevalent literature [6].

Reactions R7 and R8 represent the two primary reactions experienced by coke in the blast furnace shaft. The first order irreversible assumption is made for these reactions. The kinetic diffusion model was applied to simulate chemical reactions at the lump coke inner surface [7]. The reaction rate for a single coke particle is described by Eq. 9.

$$R_i = \frac{4}{3}\pi r_p^3 \rho_i' \eta_1 A \quad (\frac{kg\,C}{s}) \quad , i = 7,8 \quad \text{Eq. 9}$$

The intrinsic chemical reaction rate is:

$$A = \rho_p A_g k_i \frac{RT}{M_r} \quad \text{Eq. 10}$$

Where ρ_p is the apparent density of the coke, A_g is the specific internal surface area of a given coke particle (assumed to be constant during reactions), and M_r is the molecular weight of reactant gas.

The diffusion rate is expressed as:

$$B = \frac{D_e}{r_p^2} \quad \text{Eq. 11}$$

Where r_p is the radius of the coke particle and D_e is the effective diffusion coefficient in the coke pores. The Thiele modulus is defined as:

$$\Phi = \frac{reaction\ rate}{internal\ diffusion\ rate} = \sqrt{\frac{A}{B}} \quad \text{Eq. 11}$$

The effectiveness factor without the gas film mass transfer is $\frac{3}{\Phi^2}[\frac{\Phi}{\tanh(\Phi)} - 1]$. The modified effectiveness factor that includes gas film resistance is:

$$\eta_1 = \frac{\eta}{1 + \frac{\Phi}{3} \times \frac{\frac{1}{\tanh(\Phi)} - \frac{1}{\Phi}}{Bi}} \quad when\ \Phi \leq 100 \quad \text{Eq. 12}$$

and $\eta_1 = \frac{1}{\Phi}$ *when* $\Phi > 100$

Where Bi is the mass transfer Biot number [8].

The effects of CO on chemical reaction constants are defined for reaction R7 as [9]:

$$k_7 = \frac{k_{co_2}}{1 + k_{co} P_{co}}. \qquad \text{Eq. 13}$$

The effect of H_2 on k_8 is assumed to be negligible and has such, $k_8 = k_{H2O}$ for reaction R8 [10]. It is also assumed that there is no reaction of coke when its temperature is lower than 700 °C.

Reaction R9 (flux decomposition) depends heavily on the pressure at which the reaction occurs. Additionally, the URC model is applied to this reaction. Reaction R10 is assumed to reach an equilibrium point above 1273 K [11]. Above the lower boundary of the cohesive zone, the direct reduction of solid FeO takes place in two steps, via reactions R3 and R7 or reactions R6 and R8 [12]. Due to this, direct reduction of solid FeO is not explicitly simulated. However, it is implicitly covered by the gas-solid reactions R3, R7, R6 and R8. Additionally, below the cohesive zone, the reactivity of coke increases and there is no significant amount of either H_2O or CO_2 present [13].

Results

Operating conditions from a previous research project were utilitized to conduct all simulations in this study. Furance size, productivity, and injected fuel rates were obtained from previously published work. The baseline case used in this project was validated against industrial data in a previous study [4].

Effects of Coke Porosity

The initial coke bed porosity for the baseline case is 0.45. To investigate the effects of coke porosity on furnace operation, simulations were run at coke porosity values varying by ±10% and ±20%. As the coke porosity increases, gas flow experiences less resistance in the shaft. As a result, pressure drop over the furnace falls and reduction gases have a lower residence time in the shaft. These higher flow velocities result in more rapid coke consumption through gas reactions, which in turn leads to a higher coke rate and average top gas temperature as shown in the left side of Figure 1. The right side of Figure 1 shows that the top gas CO utilization decreases as the coke porosity increases. H_2 utilization is also inversely proportional to the coke bed porosity.

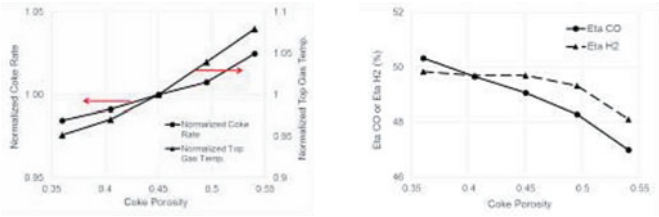

Figure 1. Coke rate and top gas average temperature vs. coke porosity (left) and CO and H_2 utilization vs. coke porosity (right)

The aforementioned variations in operating conditions at different coke bed porosities also result in a change in the shaft of the cohesive zone. As the coke bed porosity increases, the top of the cohesive zone rises, corresponding to the increased gas temperatures in the center of the furnace. The variation between cohesive zone shapes is shown in Figure 2.

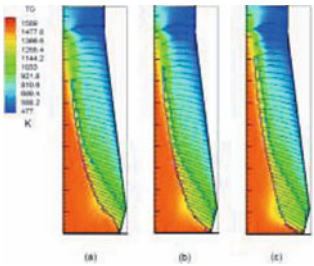

Figure 2. Contours of gas temperature for the -20% (a), baseline (b), and +20% (c) porosity cases. The cohesive zone is outlined in blue in each case.

Effects of Coke Particle Size

Coke particle size impacts furnace operation in a similar fashion. An increase in the size of coke particles leads to a higher void fraction in the coke bed. The left side of Figure 3 shows the effect of coke particles size on the coke rate and the top gas average temperature. In a similar vein to the results observed in the coke porosity cases, the coke rate and top gas average temperature both increase as the coke particle diameter increases. The top gas CO utilization falls as the coke particle diameter increases. However, the utilization of H_2 is inversely proportional to the particle size, as seen in Figure 3.

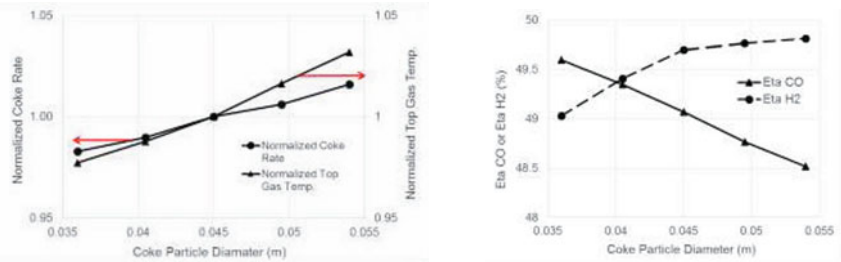

Figure 3. Coke rate and top gas average temperature vs. coke particle diameter (left) and CO and H_2 utilization vs. coke particle diameter (right)

Effects of Ore Particle Size

Iron ore particle size has a slightly different impact on the reactions inside the furnace shaft. Similar to the impact of coke particle size, an increase in ore particle size decreases the total porosity in the burden, allowing for higher velocity gas flow. However, as seen in Figure 4, the furnace coke rate remains relatively similar across all cases, while the top gas temperature experiences a steady decrease. Similar to the variation of coke particle size, increasing ore particle

size appears to have a negative impact on the utilization of CO and a slightly positive impact on the top gas H_2 utilization. This is likely due to the lower more rapid gas flow through the furnace bed as the particle size increases. Additionally, larger ore particles present a larger interfact at which reactions can occur.

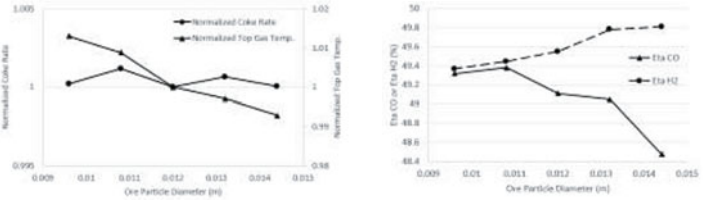

Figure 4. Coke rate and top gas average temperature vs. iron ore particle diameter (left) and CO and H_2 utilization vs. iron ore particle diameter (right)

Effects of Burden Descent Speed

The final parameter varied in this study was the burden descent speed. The rate at which burden descends through the furnace is dependent on the operating conditions below the furnace shaft. As such, it is not a direct input from furnace operators, but a burden that descends at differing speeds at along the furnace radius can lead to varied gas flow configurations and undesireable furnace operation. The burden descent speed parameter is defined as the ratio of the descent speed of the burden at the furnace center to the descent speed of the burner near the wall. Cases were run at descent speed ratios of 0.6, 0.7, 0.8 (baseline), 0.9, and 1.0. Figure 8 shows that as the rate of the descent speed is increased to 1, the coke rate reduces. As the descent speed ratio trends toward unity, the coke rate and top gas temperature decrease. Additionally, the pressure drop across the furnace increases as the ratio nears unity.

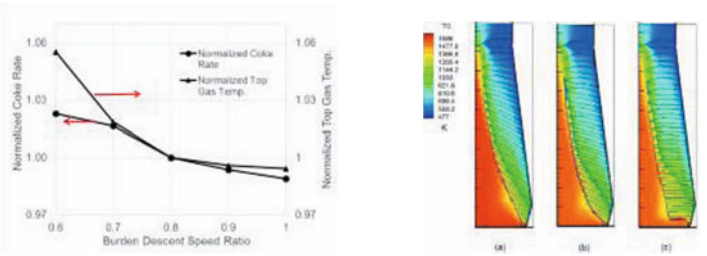

Figure 5. Coke rate and top gas average temperature vs. burden descending speed (left) and Contours of gas temperature for the 0.6 (a), baseline (b), and 1.0 (c) descent speed ratio cases (right).

The primary difference between these cases is the shape and location of the cohesive zone, shown by the blue outline in the right side of Figure 5. The radically different cohesive zones generated by varying the burden descent speed ratio change the flow patterns of gas through the packed bed of the furnace. The lower part of the cohesive zone becomes thicker as the burden descent speed ratio nears unity.

Table I details the coke rates and shaft pressure drops for each case simulated in the parametric study. In all the cases simulated, decreases in coke rate correspond to increases in the shaft pressure drop. In order to find an optimal operating condition for the furnace, both the pressure drop and the coke rate must be taken into account. Regardless of how much a given parameter can reduce the coke rate, if enough wind cannot be supplied to operate the furnace at the given conditions, it will be unfeasible as an optimization measure.

Table I. Tabulated results of comparative parametric studies

	Normalized Coke Rate	**Normalized Pressure Drop**
Coke Porosity		
-20%	0.984	1.328
-10%	0.991	1.174
Baseline (0.45)	1	1
+10%	1.007	0.892
+20%	1.025	0.764
Coke Particle Size		
0.036 m	0.983	1.174
0.041 m	0.99	1.062
Baseline (0.045 m)	1	1
0.05 m	1.006	0.965
0.054 m	1.016	0.946
Ore Particle Size		
0.0144 m	1	0.942
0.0132 m	1.001	0.976
Baseline (0.012 m)	1	1
0.0108 m	1.001	1.012
0.0096 m	1	1.022
Descent Speed Ratio		
0.6	1.023	0.965
0.7	1.017	0.988
Baseline (0.8)	1	1
0.9	0.994	1.1
1	0.989	1.135

Conclusions

The effects of coke particle size, coke bed porosity, and burden descent speed on blast furnace operation have been investigated. Coke porosity and coke particle size had, as expected, similar impacts on furnace. A 20% decrease in coke porosity resulted in a coke rate reduction of 1.6%, while a 20% increase in coke porosity resulted in a coke rate increase of 2.5%. Similarly, decreasing coke particle size resulted in up to a 1.7% coke rate reduction, while increasing the particle size resulted in a coke rate increase of 1.6%. Changing the ore particle size had little to no effect on the furnace coke rate in the ±20% range selected and presented only minor impacts on top gas temperature and pressure drop. Varying the burden descent speed ratio caused a significant change in the furnace coke rate, with a calculated coke rate reduction of 1.1%. It is important to note, however, that in all cases a reduction in the furnace coke rate corresponded to higher pressure drops (up to 33% more than baseline) over the furnace shaft. Because of this, it is necessary to take into account the wind rate that must be supplied by the blast if operation at conditions generating higher pressure drops is desired.

Acknowledgements

This research was supported by the American Iron and Steel Institute (AISI) and the U.S. Department of Energy (DOE) under Award No. DE-FG36-07GO17041. The authors would like to thank the support from the collaborators at ArcelorMittal-USA, ArcelorMittal-Dofasco, SeverStal, US Steel, US Steel - Stelco Inc., and Union Gas.

References

1. Y. H. Dang, S. M. Zhang, "Discussion on Low Fuel Rate and High PCI Rate of Blast Furnace Operation," *Iron and Steel*, 40 (2) (2005).
2. J. A. De Castro, H. Nogami, J. Yagi, "Numerical investigation of simultaneous injection of pulverized coal and natural gas with oxygen enrichment to the blast furnace," *ISIJ International*, 42 (11) (2005), 1203-1211.
3. D. Fu, Y. Chen, C. Q. Zhou, "Application of the Blast Furnace Shaft CFD Simulator," *Baosteel Academic Steel Conference 2013*, Shanghai, China, 10.
4. D. Fu, Y. Chen, C. Q. Zhou, "CFD Investigation of the Effects of Iron Ore Reducibility and Coke Reactivity on Blast Furnace Operation," *Proceedings of AISTech 2014*, Indianapolis, U.S.A., 9.
5. T. Murayama, Y. Ono, Y. Kawai, "Step-Wise Reduction of Hematite Pellets with CO-CO_2 Gas Mixtures," *Tetsu-to-Hagané*, 63 (7) (1977), 1099-1107.
6. Q. T. Tsay, W. H. Ray, J. Szekely, "The Modeling of Hematite Reduction with Hydrogen Plus Carbon Monoxide Mixtures: Part I. The Behavior of Single Pellets," *AIChE Journal*, 22 (6) (1976), 1064-1072.
7. The Iron and Steel Institute of Japan, *Blast Furnace Phenomena and Modelling* (New York, NY: Elsevier Applied Science Publishers LTD, 1987), 108-116.
8. J. B. Rawlings, J. G. Ekerdt, *Chemical Reactor Analysis and Design Fundamentals* (Madison, WI: Nob Hill Publishing, 2002).
9. S. Kobayashi, Y. Omori, "The Chemical Reaction Rate of the Solution Loss of Coke," *Tetsu-to-Hagané*, 63 (1977), 1081-1089
10. N. Miyasaka, N., S. Kondo, "The Rate of Cokes Gasification by Gas Consisting of CO_2, H_2O, CO, H_2, and N_2," *Tetsu-to-Hagané*, 54 (1968), 1427-1431.
11. H. Kokubu et al., "Effect of Humidified Blast on Blast Furnace Operation from the Viewpoint of the Softening and Melting Process of Ore Burdens," *Tetsu-to-Hagané*, 68 (15) (1982), 2338-2345.
12. W-K. Lu, "Chemical Reactions in the Blast Furnace as it Happens," *Proceedings of AISTECH 2004*, Volume I & II, 395-407.
13. G. Danloy, C. Stolz, "Shape and Position of the Cohesive Zone in a Blast Furnace," *Ironmaking Conference Proceedings*, 50 (1991), 395-407.
14. D. J. Harris, I. W. Smith, "Intrinsic Reactivity of Coke and Char to Carbon Dioxide, Steam, and Oxygen," *Twenty-Third Symposium (International) on Combustion*, 23 (1) (1991), 1185-1190.